

A Detailed Analysis of Six-Pulse Converter Harmonic Currents

David E. Rice, *Member, IEEE*

Abstract—Classical methods for the determination of six-pulse converter harmonic currents often do not adequately describe the harmonic current magnitudes actually found in practice. To accurately determine the magnitude of characteristic converter harmonics, a calculation procedure which takes into account the ripple of the dc current reflected back into the ac line current must be performed. Various methods from the literature for the determination of six-pulse converter harmonic currents are compared and a method which takes the Fast Fourier Transform of the time domain equations is described. Evaluation of these ripple effects tends to increase the magnitude of the 5th harmonic while decreasing the magnitudes of higher order harmonics. Non-characteristic harmonic orders or frequencies will sometimes also be encountered. These orders typically will be less than the 5th and can be of concern because of possible coincidence with 5th harmonic filter anti-resonance points.

I. INTRODUCTION

INDUSTRIAL power systems in recent years have experienced a tremendous growth in the application of solid-state power converters. Most of these converters utilize SCR's or diodes in a six-pulse bridge configuration. There has also been a proliferation of technical papers and seminars dealing with the ac current and voltage waveform distortion issues associated with the application of power converters. These issues have commonly been classified as the subject of harmonics due to the method of analysis of these distorted waveforms. Any distorted, periodic waveform can be segregated into a fundamental sinusoidal waveform plus a series of sinusoidal waveforms that have frequencies that are integral multiples of the fundamental. These integral multiple waveforms are *harmonics* of the fundamental quantity which can be a voltage or current.

In harmonic analysis, converters are modeled as harmonic current sources which inject harmonic currents into the ac power system. The resultant harmonic distortion of the voltage waveform can be determined according to Ohm's law. The magnitude of each harmonic voltage will be equal to the magnitude of the injected harmonic current multiplied by the harmonic impedance of the power system.

The writer has had the opportunity to conduct harmonic voltage and current measurements at a number of different industrial facilities and analytically model these same systems. In general it has been found that the harmonic calculations can

Paper PID 93-22, approved by the Petroleum and Chemical Industry Committee of the IEEE Industry Applications Society and presented at the 1992 Petroleum and Chemical Industry Committee Technical Conference. Manuscript approved for publication May 27, 1993.

The author is with General Electric Company, I&SE, Houston, TX 77080 USA.

IEEE Log Number 9214143.

be correlated quite well with field measurements. Modeling the harmonic impedances of power system components is the most difficult aspect of the analysis. However, industrial systems are physically compact and normally the impedance networks are dominated by transformers which are relatively easy to accurately model. The only significant amounts of capacitance usually present are power factor correction capacitors which are straightforward to identify and model.

Unlike the harmonic impedances of power system components, harmonic currents can easily be directly measured. In doing so it has often been found that the measured magnitudes of converter harmonic currents differ, sometimes substantially, from what have been the classic assumptions in the literature. These differences are primarily in the *magnitudes* of harmonic currents but sometimes in the *harmonic orders* as well. This paper reviews some of the classical assumptions with regard to the nature of six-pulse bridge converter harmonic currents. Some of the more recently developed methods which more closely conform to actual converter performance are reviewed. These approximate methods are compared to a more precise algorithm easily implemented with computer software. The algorithm solves the simple differential equation associated with the current waveform, and calculates the Fast Fourier Transform (FFT) of the waveform to derive the constituent harmonics.

In order to not interrupt the flow of the paper, the equations associated with the various calculation methods are contained in an appendix to this paper.

II. HARMONIC SOURCE I/H CURRENT MODEL

The abundant literature on harmonics almost without exception cite equations (1) and (2) as the means to determine the order and magnitude of the harmonic currents drawn by a six-pulse converter.

$$h = 6k \pm 1, \quad k = 1, 2, 3, \dots \quad (1)$$

$$\frac{I_h}{I_1} = 1/h \quad (2)$$

The use of (1) results in harmonic orders or multiples of the fundamental frequency of the 5th, 7th, 11th, 13th etc., and assuming a 60 hertz fundamental, correspond to 300, 420, 660 and 780 Hz respectively. The magnitude of the harmonics in per unit of the fundamental is simply the reciprocal of the harmonic order or 0.20 or 20.0% for the 5th, .143 or 14.3% for the 7th, etc. The characteristic harmonics in (1) and (2) are obtained if one performs a Fourier series calculation on the square wave or stepped square wave current illustrated

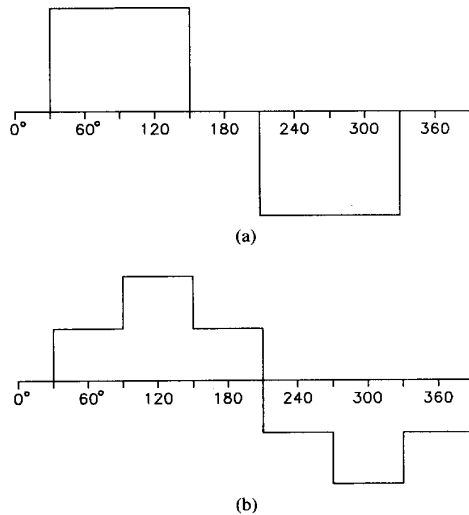


Fig. 1. (a) Idealized converter current waveform for delta-delta transformer. (b) Idealized converter current waveform for delta-wye transformer.

in Fig. 1. The stepped square wave results when a delta-wye transformer is connected between the converter terminals and the point at which the current is observed. The Fourier analysis for either wave is identical in derived harmonic magnitudes, though shifted in phase angle.

Equation (1) is a fairly good description of the harmonic orders generally encountered, although exceptions to this are discussed later in this paper. The magnitude of actual harmonic source currents have been found to often differ from the relationship described in (2). The $1/h$ values have often been described as theoretical maximums and that in practice all harmonic magnitudes are somewhat lower. The method by which these somewhat lower values are arrived at has been identified in this paper as "Classical" analysis.

III. CLASSICAL HARMONIC CURRENT SOURCE MODEL

Classical analysis can be described as the harmonics derived from a half-wave symmetrical waveform which is a perfect square wave over 120 degrees of a 180 degree half-cycle except where sloped to account for commutation effects.

Perfect square waves are clearly never encountered in actual power systems. The first step in classical analysis for modifying the values that are obtained from (2) is the recognition that a current wave cannot instantaneously change from zero to some finite magnitude as depicted in Fig. 1. In a three-phase bridge circuit there will be a period of time in which the current must commute or switch from one SCR to another. The current will decrease in one SCR while it increases in the other. The electrical angle which corresponds to this commutation time is known as the commutation angle or angle of overlap as is denoted by μ . The length of this commutation period is a function of the magnitude of the ac system inductance and the angle of SCR phase retard or firing angle. The ac system inductance is normally expressed as a pu or percent reactance on the converter rated kVA and is

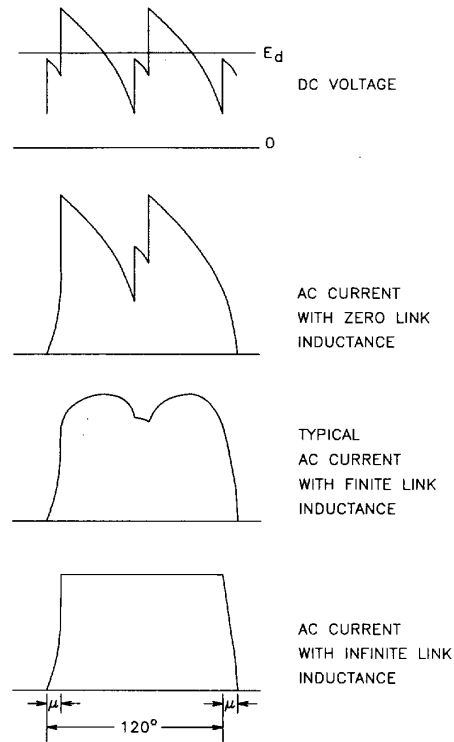


Fig. 2. Alterations in current waveform with differences in magnitude of converter output inductance.

known as the commutating reactance. This value is directly proportional to the inverse of the three phase short-circuit current available. (This ignores the effect of any capacitors which may be present which are normally not assumed to contribute to fault currents, but do provide a low impedance commutating reactance path.) A "stiff" system relative to the size of a converter results in a low value of commutating reactance while a large converter on a "weak" system will result in a high commutating reactance. The commutation angle also varies conversely with the firing angle. Higher SCR firing angles result in lower commutation angles.

The effect of the commutation angle is to slope off the vertical portions of the square wave as illustrated in Fig. 2, lowering the percentage harmonic currents from those derived from a $1/h$ calculation. Sloping of the vertical portion of the square wave attenuates the higher order harmonics in particular. The data in Table I illustrates this effect. Harmonic current percentage values are compared for two different firing angles and therefore angles of overlap. There is not a dramatic difference between the two cases for the lower order harmonics dominated by the 5th and 7th. However, the firing angle difference has a large effect on the magnitude of the higher order harmonics. The 19th is only 1.53% of the fundamental for a 10 degree firing angle, while it increases to a much more significant 4.64% value at a 60 degree firing angle. With the classical model, the per unit value of any harmonic for a given combination of high firing angle and low commutation reactance may approach but will never exceed the $1/h$ value.

TABLE I
HARMONIC CURRENT COMPARISON
Commutating Reactance = 8.0%
I/h in percent of the fundamental current

h	I/h		$\alpha=100^\circ$		$\mu=15.2^\circ$		$\alpha=60^\circ$		$\mu=5.2^\circ$	
	I _h (%)	I _h (%)	I _h (%)	% of I/h						
5	20.00	18.65	93.3	19.83	99.2					
7	14.29	12.44	87.1	14.05	98.3					
11	9.09	6.37	70.1	8.72	95.9					
13	7.69	4.62	60.0	7.26	94.4					
17	5.88	2.29	38.9	5.32	90.5					
19	5.26	1.53	29.1	4.64	88.2					
23	4.35	0.63	14.5	3.61	83.0					
25	4.00	0.51	12.8	3.21	80.3					

The real concern is the actual amps of harmonic current injected into the power system. Since the harmonic current values in Table I are in percent of the fundamental current, it is imperative that in addition to the determination of converter percentage harmonics, the converter fundamental operating current be obtained for potential worst case operating conditions.

For a constant torque drive or a constant current SCR rectifier, the converter ac current and kVA demand will remain constant as the dc voltage is lowered. The worst case for harmonics will be at whatever firing angle corresponds to minimum voltage for the application. For a variable torque application the fundamental load will tend to drop off faster than the per unit harmonics will increase with advanced firing angle. Consequently, the highest magnitude actual injected harmonic amps for at least the lower order harmonics will tend to be at the minimum firing angle corresponding to full load, full voltage conditions.

IV. HARMONIC CURRENT SOURCE MODELS INCORPORATING RIPPLE

While the current harmonics produced by some converter systems conform to the Classical model, many do not. A *critical assumption of the classical model is that there is infinite inductance on the dc output of the converter*. With this assumption, once commutation has been achieved, the current wave will be perfectly flat-topped. This is an assumption that often does not conform to the reality of how converter systems are designed and built.

A six-pulse bridge rectifier does not inherently produce a smooth, ripple-free dc voltage. The dc output voltage will have a pronounced ripple as illustrated at the top of Fig. 2, especially as the firing angle increases. The characteristic shape of the ac load current is dependent on the converter output circuit characteristic. Fig. 2 illustrates the response of the ac current to the impressed dc voltage for various values of inductance on the converter output. The ripple current in an inductive circuit will equal $1/L$ times the integral of the ripple voltage. With infinite inductance the ripple current is zero and the flat-top wave of Fig. 1 and or the bottom of Fig. 2 results. However, with some finite inductance, a ripple current of some magnitude will be impressed on the dc current. This rippled or double-humped current will be reflected in the converter input

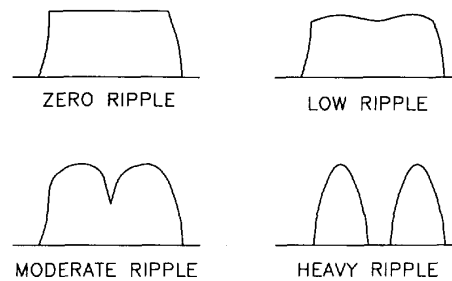


Fig. 3. Typical ripple classification.

ac current and can result in a significantly different distribution of harmonics magnitudes than those determined by classical analysis. The general effect of this double-hump is that the magnitude of the 5th harmonic current can go considerably higher than the 20% maximum predicted by classical analysis, while the higher order harmonics tend to be of much lower magnitude.

Some converter systems are equipped with a dc inductor sufficiently large that the converter responds fairly close to the classical model. This is the case with 460 volt and medium voltage current commutated induction motor drive systems, and often is true for large electrochemical rectifier units and large synchronous motor load commutated inverters. However, in some cases for the latter two systems and for dc drives, the converter output inductance is much less than infinite, to the point that the flat topped current wave assumption is no longer valid and considerable ripple exists in the current reflected to the ac line. Fig. 3 illustrates typical ac waveforms which can be encountered. It is even possible for the ripple to get so bad that the double-humps separate into two separate bumps for each half-cycle. (Note: Some ac drive systems utilize a dc link filter consisting of a link capacitor in addition to an inductor. The ac harmonics resulting from this link filter arrangement is outside the scope of this paper, as are PWM drives.)

Two methods have been proposed in the literature for the harmonic analysis of these complex double-humped waveforms. Methods by Dobinson and Graham-Schonholzer are summarized in an appendix to this paper. The latter method is included in the latest IEEE 519 Standard [3]. Both methods require that the ripple ratio r or the ripple coefficient r_c be known. In order to calculate either of these terms, the integral of the ripple voltage must be determined. A method given by Schaefer [4] to obtain this critical factor has been summarized in the appendix. Although somewhat complex, the equations for all these methods can be fairly easily incorporated into a spreadsheet for rapid calculations given the powerful personal computers now available. Both time domain waveforms as well as harmonic spectrums can be calculated and graphed.

The Dobinson and Graham-Schonholzer methods are both approximations since it is assumed that the double-humps represent portions of sinusoidal waveforms. Furthermore, the Dobinson method does not take into account waveform sloping due to commutation. Refer to Table II for a summary of the features of each algorithm discussed in this paper. An

TABLE II
HARMONIC CURRENT CALCULATION METHOD COMPARISON
(1) G-S uses straight line approximation for current waveform sloping due to commutation. (2) Dobinson and G-S use sine wave top approximations to represent ripple.

Method	Commutation Angle	Ripple
1/h	NO	NO
Classical	YES	NO
Dobinson	NO	YES (Approx.)
Graham-Schonholzer	YES (Approx.)	YES (Approx.)
FFT	YES	YES

additional more exact method was derived for this paper and is described in the appendix as the "FFT Method." The term "FFT Method" is a convenient label but it does not adequately describe the process by which the current harmonics of an SCR converter are determined. A software implemented numerical analysis procedure is utilized to describe the current wave in the time domain. Rather than using a single $(1/L) \times$ Integral of voltage quantity applicable twice each half cycle and assuming sine wave shaped humps as in the other methods, an incremental step-by-step integration procedure constructs the actual current wave. Once the time domain current function is established, a FFT (Fast Fourier Transform) can easily be performed via computer software to arrive at the constituent harmonics.

While a rigorous comparison with actual field measurements was not conducted, the FFT method seemed to offer much more realistic harmonic current magnitudes that those derived by other methods across a complete range of converter characteristics.

V. A COMPARISON OF HARMONIC SOURCE MODELS

The performance of the 1/h, Classical, Dobinson and Graham-Schonholzer calculation methods relative to the FFT method is summarized in Table III. All calculations were based on a converter with an Edo of 2850 volts, corresponding to a 2100 volt input ac line-to-line voltage, and a dc current loading of 1000 amps. Cases were run with variations in three different parameters. The commutation reactance was set at either 12.0%, 8.0% or 1.0%. Firing angles of 10 degrees, (typical minimum SCR firing angle), 25 degrees and 60 degrees were examined. Cases were run for a relatively large link inductor of 6.5 mH, a moderate size of 1.5 mH and a low value of 0.5 mH. All combinations of these parameters yielded the twenty-seven cases summarized in Table III. The actual harmonic current listings for nine of the twenty-seven cases are shown in Table IV, (all cases with $X_c = 8.0\%$.)

The weighted average standard deviation numbers in Table III are an indication on the accuracy of the harmonic currents obtained from the other methods to those obtained from the FFT method. This number was calculated by first taking the standard deviation of every characteristic harmonic from the 5th to the 49th between the FFT method and the other method being evaluated. The average of these standard deviations for all the harmonics was then calculated after applying a weighting factor of 1/h. The weighting factor was to allow for the fact that the lower order, higher magnitude harmonics

TABLE III
SUMMARY OF WEIGHTED STANDARD DEVIATIONS FROM THE
FFT METHOD OF THE OTHER CALCULATION TECHNIQUES

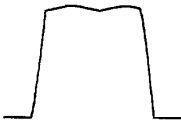
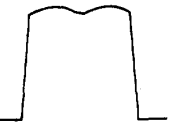
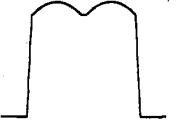
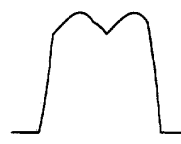
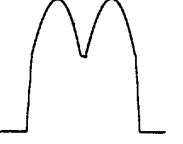
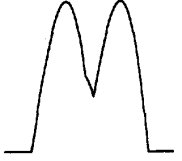
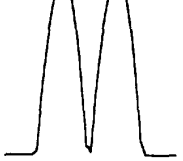
Case	-- Conditions --			Weighted Standard Deviations (Relative to FFT Method)			
	Link mH	pu Xc	Firing Angle				
				1/h	Classic	Dobinson	G-S
1	6.5	0.12	10	1.591	0.151	1.569	0.797
2	6.5	0.08	10	1.196	0.164	1.174	0.825
3	6.5	0.01	10	0.225	0.147	0.089	0.973
4	6.5	0.12	25	1.121	0.294	1.034	0.760
5	6.5	0.08	25	0.889	0.314	0.673	0.806
6	6.5	0.01	25	0.339	0.322	0.020	0.886
7	6.5	0.12	60	1.044	0.593	0.516	0.713
8	6.5	0.08	60	0.857	0.624	0.289	0.717
9	6.5	0.01	60	0.652	0.648	0.014	0.680
Average Cases 1-9				0.879	0.362	0.598	0.795
10	1.5	0.12	10	1.737	0.630	1.453	0.630
11	1.5	0.08	10	1.605	0.699	1.076	0.618
12	1.5	0.01	10	0.712	0.634	0.135	0.673
13	1.5	0.12	25	2.065	1.250	0.935	0.379
14	1.5	0.08	25	1.915	1.344	0.594	0.316
15	1.5	0.01	25	1.401	1.384	0.036	0.148
16	1.5	0.12	60	2.972	2.526	0.681	0.500
17	1.5	0.08	60	2.895	2.662	0.435	0.749
18	1.5	0.01	60	2.766	2.762	0.029	1.339
Average Cases 10-18				2.008	1.543	0.597	0.595
19	0.5	0.12	10	2.704	1.666	1.384	1.118
20	0.5	0.08	10	2.746	1.872	1.109	1.086
21	0.5	0.01	10	1.858	1.780	0.412	0.960
22	0.5	0.12	25	3.469	2.697	0.864	2.806
23	0.5	0.08	25	3.489	2.933	0.763	3.436
24	0.5	0.01	25	3.209	3.192	0.253	4.972
25	0.5	0.12	60	4.962	4.627	1.096	41.573
26	0.5	0.08	60	5.016	4.820	0.818	248.425
27	0.5	0.01	60	4.369	4.365	0.879	30.647
Average Cases 19-27				3.536	3.106	0.842	37.225

such as the 5th and the 7th are generally of more importance in harmonic evaluation. For example, the 5th has seven times the influence as the 35th in the results summarized in Table III with this evaluation procedure.

For the cases with the relatively large 6.5 mH link inductor, the classical method actual performs fairly well on an overall basis. Even with this size inductor there is some current ripple so the classical method tends to undershoot the 5th somewhat, especially as the firing angle increases. However, it does a very good job on the higher order harmonics since it represents the commutation sloping effects which tend to attenuate the higher orders. Dobinson essentially assumes a zero degree commutation angle so this method appreciably overshoots on the higher order harmonics which actually are quite attenuated at retarded firing orders. It tends to also overshoot on the 5th but not to as great a degree. Graham-Schonholzer on the other hands tends to undershoot harmonic magnitudes, especially for the 5th at lower firing angles.

With the moderate 1.5 mH inductor, Dobinson and Graham-Schonholzer come into their own with their modeling of the current humps. Dobinson models the 5th quite well but overshoots on the higher orders, especially at minimum firing angle. Graham-Schonholzer does quite well at retarded firing

TABLE IV
HARMONIC CURRENTS CALCULATED FOR VARIOUS METHODS (ONLY CASES WITH Xc = 0.08 pu.)

<p>CASE 2</p> <p>L = 6.50 mH Xc = 0.08 pu Alpha = 10.00 deg Overlap = 15.20 deg</p> 						<p>CASE 5</p> <p>L = 6.50 mH Xc = 0.08 pu Alpha = 25.00 deg Overlap = 9.28 deg</p> 						<p>CASE 8</p> <p>L = 6.50 mH Xc = 0.08 pu Alpha = 60.00 deg Overlap = 5.17 deg</p> 					
h	1/h	Classical	Dobinson	GS	FFT	h	1/h	Classical	Dobinson	GS	FFT	h	1/h	Classical	Dobinson	GS	FFT
5	20.000	18.653	20.849	15.718	19.436	5	20.000	19.462	21.270	17.061	20.842	5	20.000	19.831	22.331	18.995	22.445
7	14.286	12.440	13.338	8.810	11.664	7	14.286	13.539	12.868	9.531	12.028	7	14.286	14.050	11.683	9.319	11.112
11	9.091	6.373	9.081	4.767	6.241	11	9.091	7.945	9.076	6.327	7.826	11	9.091	8.723	9.064	7.279	8.621
13	7.692	4.618	7.302	3.321	4.485	13	7.692	6.359	7.108	4.678	5.874	13	7.692	7.260	6.619	5.149	6.133
17	5.882	2.292	5.812	1.464	2.180	17	5.882	4.206	5.777	3.235	4.026	17	5.882	5.324	5.689	4.265	5.054
19	5.263	1.526	5.029	0.977	1.540	19	5.263	3.434	4.912	2.582	3.245	19	5.263	4.643	4.619	3.389	4.036
23	4.348	0.627	4.274	0.035	0.609	23	4.348	2.254	4.238	1.682	2.111	23	4.348	3.610	4.146	2.830	3.355
25	4.000	0.513	3.835	0.111	0.501	25	4.000	1.795	3.753	1.373	1.734	25	4.000	3.206	3.547	2.381	2.837
29	3.448	0.617	3.380	0.471	0.623	29	3.448	1.069	3.346	0.762	0.975	29	3.448	2.547	3.261	1.966	2.332
31	3.226	0.654	3.100	0.470	0.619	31	3.226	0.784	3.037	0.609	0.785	31	3.226	2.274	2.879	1.712	2.041
35	2.857	0.612	2.796	0.467	0.595	35	2.857	0.343	2.765	0.199	0.295	35	2.857	1.811	2.688	1.380	1.638
37	2.703	0.545	2.601	0.411	0.532	37	2.703	0.188	2.550	0.129	0.210	37	2.703	1.613	2.423	1.229	1.467
41	2.439	0.366	2.383	0.241	0.348	41	2.439	0.161	2.356	0.125	0.180	41	2.439	1.270	2.286	0.955	1.135
43	2.326	0.274	2.240	0.182	0.278	43	2.326	0.236	2.198	0.148	0.201	43	2.326	1.120	2.091	0.864	1.032
47	2.128	0.145	2.077	0.002	0.143	47	2.128	0.347	2.052	0.278	0.346	47	2.128	0.858	1.989	0.635	0.757
49	2.041	0.141	1.968	0.039	0.135	49	2.041	0.379	1.931	0.275	0.345	49	2.041	0.743	1.840	0.581	0.696
<p>% HDF 30.015 23.971 29.915 19.038 24.130</p> <p>Wtg SD 1.196 0.164 1.174 0.825 0.000</p>						<p>% HDF 30.015 26.564 29.888 21.607 26.665</p> <p>Wtg SD 0.889 0.314 0.673 0.806 0.000</p>						<p>% HDF 30.015 28.537 29.892 24.147 28.604</p> <p>Wtg SD 0.857 0.624 0.289 0.717 0.000</p>					
<p>CASE 11</p> <p>L = 1.50 mH Xc = 0.08 pu Alpha = 10.00 deg Overlap = 15.20 deg</p> 						<p>CASE 14</p> <p>L = 1.50 mH Xc = 0.08 pu Alpha = 25.00 deg Overlap = 9.28 deg</p> 						<p>CASE 17</p> <p>L = 1.50 mH Xc = 0.08 pu Alpha = 60.00 deg Overlap = 5.17 deg</p> 					
h	1/h	Classical	Dobinson	GS	FFT	h	1/h	Classical	Dobinson	GS	FFT	h	1/h	Classical	Dobinson	GS	FFT
5	20.000	18.653	23.677	20.302	21.996	5	20.000	19.462	25.503	24.589	25.413	5	20.000	19.831	30.100	36.422	31.067
7	14.286	12.440	10.179	5.875	9.162	7	14.286	13.539	8.140	5.465	7.183	7	14.286	14.050	3.006	1.247	1.676
11	9.091	6.373	9.048	4.546	5.765	11	9.091	7.945	9.027	6.882	7.407	11	9.091	8.723	8.974	9.637	8.280
13	7.692	4.618	5.999	2.896	4.018	13	7.692	6.359	5.158	3.593	4.263	13	7.692	7.260	3.041	2.629	2.411
17	5.882	2.292	5.578	1.055	1.817	17	5.882	4.206	5.426	3.097	3.417	17	5.882	5.324	5.045	4.829	4.165
19	5.263	1.526	4.246	1.087	1.577	19	5.263	3.434	3.741	2.249	2.609	19	5.263	4.643	2.470	2.246	2.026
23	4.348	0.627	4.029	0.206	0.593	23	4.348	2.254	3.871	1.440	1.635	23	4.348	3.610	3.473	2.905	2.513
25	4.000	0.513	3.285	0.083	0.498	25	4.000	1.795	2.930	1.325	1.526	25	4.000	3.206	2.037	1.797	1.616
29	3.448	0.617	3.154	0.537	0.640	29	3.448	1.069	3.007	0.545	0.667	29	3.448	2.547	2.639	1.870	1.623
31	3.226	0.654	2.679	0.340	0.507	31	3.226	0.784	2.407	0.677	0.784	31	3.226	2.274	1.723	1.410	1.269
35	2.857	0.612	2.590	0.426	0.539	35	2.857	0.343	2.458	0.043	0.171	35	2.857	1.811	2.124	1.223	1.067
37	2.703	0.545	2.261	0.373	0.487	37	2.703	0.188	2.042	0.234	0.290	37	2.703	1.613	1.489	1.087	0.982
41	2.439	0.366	2.198	0.167	0.289	41	2.439	0.161	2.078	0.216	0.242	41	2.439	1.270	1.776	0.783	0.689
43	2.326	0.274	1.956	0.211	0.291	43	2.326	0.236	1.773	0.047	0.103	43	2.326	1.120	1.310	0.818	0.743
47	2.128	0.145	1.908	0.057	0.147	47	2.128	0.347	1.800	0.314	0.342	47	2.128	0.858	1.526	0.472	0.421
49	2.041	0.141	1.724	0.013	0.127	49	2.041	0.379	1.566	0.198	0.233	49	2.041	0.743	1.169	0.595	0.543
<p>% HDF 30.015 23.971 30.041 21.883 24.998</p> <p>Wtg SD 1.605 0.699 1.076 0.618 0.000</p>						<p>% HDF 30.015 26.564 30.495 26.725 28.201</p> <p>Wtg SD 1.915 1.344 0.594 0.316 0.000</p>						<p>% HDF 30.015 28.537 32.831 38.445 32.872</p> <p>Wtg SD 2.895 2.662 0.435 0.749 0.000</p>					
<p>CASE 20</p> <p>L = 0.50 mH Xc = 0.08 pu Alpha = 10.00 deg Overlap = 15.20 deg</p> 						<p>CASE 23</p> <p>XL = 0.50 mH Xc = 0.08 pu Alpha = 25.00 deg Overlap = 9.28 deg</p> 						<p>CASE 26</p> <p>L = 0.50 mH Xc = 0.08 pu Alpha = 60.00 deg Overlap = 5.17 deg</p> 					
h	1/h	Classical	Dobinson	GS	FFT	h	1/h	Classical	Dobinson	GS	FFT	h	1/h	Classical	Dobinson	GS	FFT
5	20.000	18.653	31.031	36.709	29.030	5	20.000	19.462	36.508	61.568	37.275	5	20.000	19.831	50.300	159.71	52.888
7	14.286	12.440	1.967	4.629	5.723	7	14.286	13.539	4.151	14.508	7.687	7	14.286	14.050	19.553	718.594	23.314
11	9.091	6.373	8.964	3.756	4.713	11	9.091	7.945	8.900	9.607	6.363	11	9.091	8.723	8.741	219.955	7.417
13	7.692	4.618	2.613	1.374	2.950	13	7.692	6.359	0.090	1.737	0.921	13	7.692	7.260	6.261	222.179	7.037
17	5.882	2.292	4.968	0.412	1.223	17	5.882	4.206	4.514	2.419	1.903	17	5.882	5.324	3.371	55.103	1.917
19	5.263	1.526	2.213	1.481	1.699	19	5.263	3.434	0.698	0.612	1.029	19	5.263	4.643	3.116	99.640	3.060
23	4.348	0.627	3.393	1.067	0.836	23	4.348	2.254	2.919	0.247	0.524	23	4.348	3.610	1.724	9.597	0.388
25	4.000	0.513	1.856	0.777	0.724	25	4.000	1.795	0.791	1.091	1.003	25	4.000	3.206	1.890	50.311	1.472
29	3.448	0.617	2.564	0.772	0.696	29	3.448	1.069	2.125	0.520	0.318	29	3.448	2.547	1.020	6.739	0.173
31	3.226	0.654	1.584	0.126	0.319	31	3.226	0.784	0.769	1.014	0.783	31	3.226	2.274	1.283	25.524	0.682
35	2.857	0.612	2.057	0.279	0.415	35	2.857	0.343	1.659	0.723	0.423	35	2.857	1.811	0.658	12.821	0.380
37	2.703	0.545	1.378	0.240	0.382	37	2.703	0.188	0.720	0.753	0.517	37	2.703	1.613	0.937	11.553	0.244
41	2.439	0.366	1.715	0.097	0.209	41	2.439	0.161	1.356	0.665	0.415	41	2.439	1.270	0.451	14.511	0.441
43	2.326	0.274	1.217	0.314	0.331	43	2.326	0.236	0.666	0.453	0.271	43	2.326	1.120	0.720	3.234	0.014
47	2.128	0.145	1.470	0.255	0.208	47	2.128	0.347	1.143	0.492	0.331	47	2.128	0.858	0.321	14.102	0.432
49	2.041	0.141	1.089	0.200	0.179	49	2.041	0.379	0.616	0.184	0.082	49	2.041	0.743	0.574	1.767	0.158
<p>% HDF 30.015 23.971 33.488 37.283 30.218</p> <p>Wtg SD 2.746 1.872 1.109 1.086 0.000</p>						<p>% HDF 30.015 26.564 38.362 64.087 38.696</p> <p>Wtg SD 3.489 2.933 0.763 3.436 0.000</p>						<p>% HDF 30.015 28.537 55.325 1778.06 58.836</p> <p>Wtg SD 5.016 4.820 0.818 248.425 0.000</p>					

angles but tends to overshoot to some degree on all orders at advanced firing angles. As expected, the classical method which assumes a flat-top wave begins to miss badly on the 5th and the 7th harmonic magnitudes.

Use of the small 0.5 mH inductor only further shows the inadequacy of the classical method as it severely undershoots the correct magnitude for the 5th. Dobinson does quite well, especially in modeling of the 5th which totally dominates the other harmonics, especially at advanced firing angles. At a 60 degree firing angle the total current wave HDF is 58.8%, of which 52.9% is the 5th. (Dobinson comes in close at 50.3%.) With the 0.5 mH inductor and the 60 degree firing angle the ripple is so severe that the humped wave separates into two bumps. It becomes clear that the Graham-Schonholzer algorithm breaks down for this condition as all harmonics severely overshoot.

In conclusion, it appears that only the FFT Method is adequate to accurately predict converter harmonics across the converter operating range and with a variety of converter output inductances. If another method is used, it appears Dobinson is conservative in that it performs well for moderate to heavy ripples and moderately overshoots for low ripple, (high link inductance) waveforms. If a mix of non-FFT methods can be used the following is suggested:

Ripple	Method to Use
Low	Classical
Moderate	Dobinson for 5th and 7th, Graham-Schonholzer for higher orders.
Heavy	Dobinson

The FFT method does a precise job of calculating constituent waveform harmonics given the limitations of the single inductance converter output network it assumes as depicted in Fig. 4. However, additional complexities could be introduced into the evaluation. A network more extensive than a single inductance could produce more accurate results where converters are utilized to drive dc motors. [5] [6] The FFT model in this paper assumes a perfectly sinusoidal ac voltage waveform at the terminals of the converter. This waveform will be distorted in proportion to the commutating reactance in the absence of any capacitance resonance effects or other converters present on the system. An iterative process could be used to further modify the current waveform based on voltage distortion of the ac system.

However, it is the writer's experience that the converter current harmonics obtained without these complexities are sufficient for most engineering evaluations and also appear to correspond quite well with actual field measurements conducted on a number of sizes and types of converter systems.

VI. SYSTEM CONSEQUENCES OF NON-CLASSICAL HARMONIC MAGNITUDES

Modeling of the harmonics resulting from the complex double-humped current wave may be complex but the net

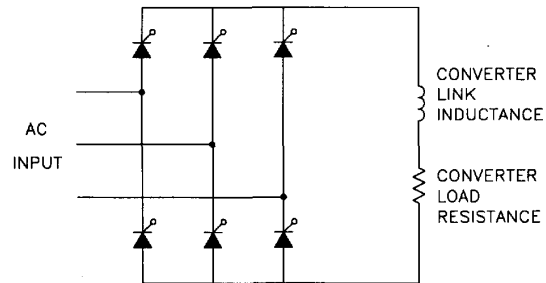


Fig. 4. Six pulse bridge rectifier model.

effect is relatively simple. A converter with high ripple will tend to have higher 5th harmonic magnitudes along with lower magnitudes for the characteristic higher order harmonics. From a power system standpoint this is not necessarily better or worse, it is just different. If there is 5th harmonic filtering present, the resulting bus harmonic distortion factor will be lower with high ripple converter systems which are putting out predominately 5th harmonic. However, the 5th harmonic duties on the filtering equipment will be greater than what they would be with a more classical harmonic current distribution and this must be allowed for in the filter design.

If 5th harmonic filtering is not present, the high magnitude and dominant 5th harmonic current injected to the utility might make it more likely that the injected harmonic current restrictions of IEEE 519 will be violated. The crucial point is that converter source harmonic currents must be evaluated in a manner which closely predicts actual experience, so that the appropriate decisions can be made for the handling of harmonic distortion on the system.

VII. NON-CHARACTERISTIC HARMONIC ORDERS

Thus far in this paper the variance of harmonic current magnitudes from classical models has been discussed while assumed the validity of the harmonic orders expressed in (2). This equation normally does describe well the harmonic orders for which six-pulse bridge converters normally produce significant harmonic current magnitudes. However, there are other harmonics orders which can be present in some circumstances that can conceivably become a problem to the power system.

VIII. EVEN ORDER HARMONICS

Refer to Fig. 5 which depicts the measured waveform and harmonic spectrum for a large 3000 hp mixer dc drive. As expected with this high ripple wave, the 5th harmonic is the highest at 26.5%. However, note the three harmonics following in order of magnitude are the 4th, 2nd and 6th at 16.3%, 15.8% and 8.6% respectively. The presence of these even harmonics is not normal. It is evident that the drive regulator is most likely improperly tuned with excessive gain which produces the asymmetry between the first and second humps in each half-cycle. This alone would not produce even harmonics. They result because the asymmetry in SCR firing results in the higher hump leading on the positive half-cycle, while it is trailing in the negative half-cycle.

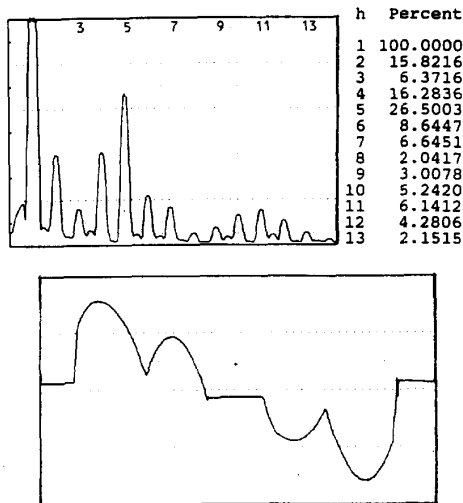


Fig. 5. DC drive current with non-half-wave symmetrical waveform resulting in significant even harmonics.

Even harmonics will be present if a waveform is not half-wave symmetrical. A wave has half-wave symmetry if $f(\omega t) = -f(\omega t + \pi)$. In graphical terms, if you take the positive half-cycle waveform, flip it about the x -axis and slide it to the right 180 degrees and are able to line it up perfectly with the negative half-cycle wave, the waveform has half-wave symmetry and no even harmonics exist. If this procedure is followed for the measured waveform in Fig. 5, it is evident that significant half-wave asymmetry exists which confirms the existence of even harmonics. In this case the drive was operating successfully with no resulting problems to the power system; however, that would not necessarily always be the case as will be discussed later in this paper.

IX. NON-INTEGER HARMONICS

The term "Non-Integer Harmonic" really is a contradiction of terms. By definition a harmonic is, "An integer multiple of some fundamental quantity". However, the terms seems to accurately describe an interesting effect which can occur in the application of ac converters on ac adjustable speed drives. Measurements were taken in a polyethylene plant that due to some unusual circumstances resulted in some very evident, though non-injurious, "Non-Integer Harmonics".

Fig. 6 depicts spectrum analyzer plots of current and voltage waveforms measured at the plant. The converter source current plot shows that in addition to the classic harmonic orders, (5th, 7th, 11th, 13th, etc.), there are two low magnitude "harmonics" at 345 Hz and to a lesser extent at 465 Hz. On a 60 hertz base these represent harmonic orders of 5.75 and 7.75. These are actually integer multiples of the *fundamental inverter running frequency* of this load commutated synchronous motor drive reflected back across the dc link and converter into the ac system. These reflected inverter harmonics typically are low magnitude, on the order of 1% to 6%, and are generated in sidebands pairs according to (3).

$$f_{SB} = 6f_I \pm f \quad (3)$$

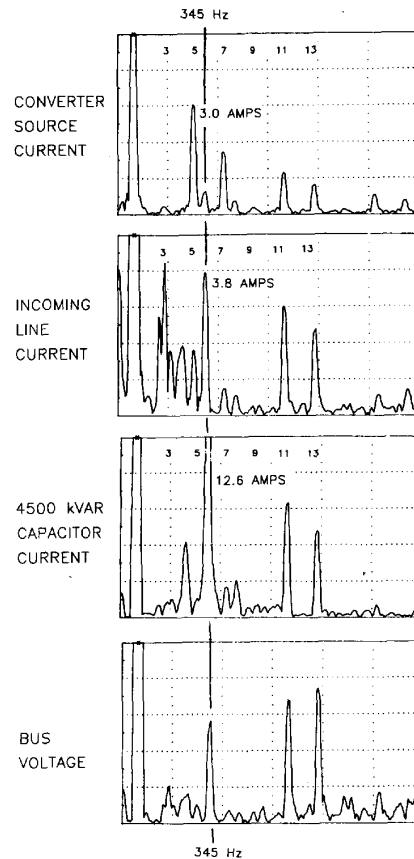


Fig. 6. Spectrum traces depicting amplification on 345 Hz non-integer harmonic.

Where: f_{SB} = Frequency of sideband harmonic
 f_I = Inverter running frequency
 f = AC system base frequency

The drive in question was actually running in excess of the base speed of 360 rpm at 405 rpm which corresponds to an inverter frequency of 67.5 hz. Equation 3 correctly computes the observed reflected inverter harmonics at 345 and 465 hertz.

X. SYSTEM CONSEQUENCES OF NON-CHARACTERISTIC HARMONIC ORDERS

The non-characteristic harmonics previously discussed are mostly orders less than the 5th. For the dc drive generating even harmonics, the 2nd and the 4th were the significant offenders. In the case of the ac drive, the non-integer harmonic orders generated were 5.75 and 7.75. However, the drive was running in excess of base speed with the inverter frequency greater than 60 hertz. For the more typical situation with the drive operating at some speed below base speed, the lower order (and higher magnitude) harmonic of the sideband pair would be at a frequency less than the fifth harmonic.

Another harmonic almost always present in power systems is the 3rd. Drives normally produce very little third, (the 6.37% magnitude of 3rd in Fig. 5 is an exception!) The presence of the third on most systems is due to transformer saturation. The magnitude of the third can go up significantly when the system is operated above rated transformer voltage as the transformer cores saturate and draw an exciting current greatly increased in both magnitude and distortion level.

The possible presence of harmonics less than the 5th order leads to special concern for the application of 5th harmonic filters. This filtering is often applied when a significant amount of load consists of six-pulse converter equipment. It is commonly understood that the presence of unfiltered or "naked" capacitors can lead to problems on a power system with harmonic generating loads. This is due to the possibility of parallel resonance of the capacitors with the inductive reactance of the power system at a frequency which corresponds to a harmonic present on the system. The result is the amplification of voltage and current distortion of the harmonic to which the parallel combination is tuned. Equation 4 is the familiar formula which expresses the parallel resonance tuning point given a system fault SCMVA available and capacitor MVARC size.

$$h_p = \sqrt{\frac{\text{SCMVA}}{\text{MVARC}}} \quad (4)$$

One justification for filtering is to remove this threat of parallel resonance. However, it must be understood that the use of a series tuning reactor on a bank of power factor correction capacitors does not *eliminate* the parallel tuning point of the capacitors. It merely shifts the parallel tuning point below the series tuning point of the filter.

The capacitor and tuning reactor combination will be capacitive below the tuning point of the filter and will have a parallel tuning point, sometimes referred to as the filter anti-resonance point, below the series tuning point. The tuning frequency of the anti-resonance point is a function of the filter size, series tuning and short-circuit MVA of the system and can be calculated using (5).

$$h_{AR} = \sqrt{\frac{1}{\frac{\text{MVARC}}{\text{SCMVA}} + \frac{1}{h_f^2}}} \quad (5)$$

A 5th filter anti-resonance point somewhere below 300 hz is usually considered to be a "safe" location. However, if the anti-resonance tuning point corresponds to a non-characteristic harmonic order present on the system, amplification of that harmonic will occur.

Filter anti-resonance tuning was a factor for the previously discussed situation with the spectrum measurements in Fig. 6. The plant was equipped with two 6.3 MVAR 5th harmonic filters on the same 13.8 kV bus feeding the ac adjustable speed drives. Due to the loss of some of the outdoor stack rack capacitor cans due to bird and/or rodent activity, one of the filter sizes was reduced to 4.5 MVAR with a resultant shift upwards of both the series tuning point and the anti-resonance point. The series tuning point was shifted up to $h = 6.33$ and the resultant filter anti-resonance point ended up at 353 hertz, very close to the 345 hertz reflected inverter

harmonic. The net result was that due to parallel resonance, 3 amps of the 5.75th produced in the drive was amplified to 12.6 amps in the capacitor, and the 5.75th was the third largest source of harmonic distortion after the 11th and 13th. (The six-pulse drives had transformer winding configurations to allow 12 pulse cancellation largely eliminating the 5th and the 7th.) The spectrum analysis plots in Fig. 6 clearly show this amplification effect.

Despite the amplification of this uncharacteristic harmonic, there were no problems on this particular system since the overall distortion level was kept very low by the 12-pulse arrangement and the filtering. Nevertheless, this situation illustrated the need for caution in the application of filtering where the presence of non-characteristic and even non-integer harmonics is a possibility.

XI. CONCLUSION

The assumption of $1/h$ per unit harmonics, even when modified to allow for the attenuating effects of commutation, will not adequately describe the actual magnitude of six-pulse converter harmonic currents in many cases. To accurately determine the magnitude of characteristic converter harmonics, a calculation procedure which takes into account the ripple of the dc current reflected back into the ac line current must be performed. Evaluation of these ripple effects will tend to increase the magnitude of the 5th harmonic while decreasing the magnitude of the higher order characteristic harmonics. The FFT method described in this paper and implemented in computer software will accurately predict converter harmonic currents across a range of firing angles, commutating reactance and dc link inductance values. The classical, Dobinson or Graham-Schonholzer methods can be implemented by hand calculation but the limitations of each must be considered or large errors in the results may occur.

Non-characteristic harmonic orders or frequencies will sometimes also be encountered. These orders typically will be less than the 5th and can be of concern because of possible coincidence with 5th harmonic filter anti-resonance points.

APPENDIX

A. Calculation Procedures

All the calculations in this appendix apply for a six-pulse double way (bridge) SCR rectifier. The same information applies to multi-pulse converters except that allowance must be made for cancellation of the appropriate harmonics.

B. Variable Definitions

α	Firing angle
$\Delta \int E_r$	Incremental ripple voltage integral for FFT method
Δi	Ripple current
$\Delta \omega t$	Angular increment for FFT method
E_d	Average dc voltage
E_{d0}	Maximum average dc voltage
E_{LL}	AC line-to-line RMS voltage

E_m	Maximum crest dc voltage
e_r	DC ripple voltage
E_r	Value of dc voltage ripple at end of integration interval
E_{r_o}	Value of dc voltage ripple at start of integration interval
f	AC system frequency
f_I	Inverter running frequency
f_{SB}	Reflected inverter sideband frequencies
h	Order of harmonic
h_{AR}	Filter anti-resonance tuning point
h_f	Filter series tuning point
h_p	Parallel resonance tuning point
$i(\omega t)$	AC current waveform as a function of ωt
I_1	Fundamental current
$I_{1_{rated}}$	Converter rated fundamental current
I_c	Commutation current
I_d	Average dc current
$I_{d_{rated}}$	Converter rated average dc current
I_h	Harmonic current
I_h/I_1	Pu harmonic current
I_r	Value of dc current ripple at end of integration interval
I_{r_o}	Value of dc current ripple at start of integration interval
I_{sc}	Three-phase fault current at converter terminals
$\int edt$	Time integral of ripple voltage (Schaefer)
μ	Commutation angle
mH	Converter output inductance in millihenries
MVARC	Three phase capacitor MVAR
r	Ripple ratio = $\Delta i/I_d$
r_c	Ripple coefficient = $\Delta i/I_c$
SCMVA	Three phase short-circuit MVA
X_c	Commutation reactance in pu

C. Classical Analysis

Classical analysis allows for harmonic attenuation due to commutation but no ripple effects are accounted for since infinite inductance on the converter output is assumed.

Harmonic magnitudes in per unit of the fundamental ac input current may be computed in accordance with (6). [2] [7]

$$\frac{I_h}{I_1} = \frac{\sqrt{a^2 + b^2 - 2ab \cos(2\alpha + \mu)}}{h(\cos \alpha - \cos(\alpha + \mu))} \quad (6)$$

Where:

$$a = \frac{\sin((h-1)\mu/2)}{h-1},$$

$$b = \frac{\sin((h+1)\mu/2)}{h+1}.$$

In order to utilize this equation the firing angle must be set and the angle of overlap computed. The SCR firing angle is determined by the dc voltage required by the load at the converter output and is expressed in (7). (In a dc drive the output voltage is proportional to speed. In an ac adjustable speed drive the drive speed is governed by the frequency of the inverter output. The volts/hertz ratio is usually kept constant so that the converter voltage will also

be proportional to the required drive speed. AC drive control strategies may be utilized at the high end of the speed range, (80%–100%), which hold voltage constant and allow the volts/hertz ratio to rise. This can be done as long as the higher flux density is acceptable to the motor design. Constant converter voltage maintains a minimum converter firing angle thereby maintaining both a higher power factor and lower ac harmonic currents.)

$$\frac{E_d}{E_{do}} = \frac{\cos(\alpha) + \cos(\alpha + \mu)}{2} \quad (7)$$

The commutating angle is a function of the firing angle and the commutating reactance X_c . The commutating reactance can be calculated using (8) which is the ratio of the converter rated ac line current divided by the available three phase fault current at the converter terminals.

$$X_c = \frac{I_{1_{rated}}}{I_{sc}} \quad (8)$$

The commutating angle can be calculated using (9).

$$\mu = \arccos(e^2 - ce + \sqrt{(ce - e^2)^2 - e^2 - c^2 + d^2 + 2ce}) \quad (9)$$

Where:

$$c = X_c \frac{I_d}{I_{d_{rated}}},$$

$$d = \sin \alpha,$$

$$e = \cos \alpha.$$

Based on the previously discussed material and equations (6) through (9), the following procedure can be followed to compute the spectrum of harmonic currents.

- 1) Calculate the commutating reactance.
- 2) Determine the required firing angle by using (7) based on the Ed required by the load assuming the commutation angle is equal to 0.
- 3) Utilize equation (9) to calculate the commutation angle given the X_c and firing angle already determined.
- 4) Calculate the resultant Ed using (7). For larger commutation angles this may lower Ed sufficiently from the desired magnitude that an iterative process may have to be used between steps b and d to arrive at a firing angle which provides the desired Ed.

Note: The iterative process is normally not required for harmonic analysis. A check at the maximum dc voltage would set the converter bridge at a minimum SCR firing angle which is about 10 degrees. The Ed resulting from this firing angle and associated commutation angle is the maximum and cannot be raised. When the harmonics are checked at maximum firing angles, (minimum operating dc voltage), the commutation angles get very small and the pu Ed varies little from $\cos(\alpha)$.

- 5) Once the setpoint firing angle and resulting angle of overlap have been determined the spectrum of harmonic currents can be calculated using (6).

D. Calculation of DC Current Ripple

The dc current ripple is an input variable vital to the computation of harmonics according to the Dobinson or Graham-Schonholzer methods. The following equations derived from Schaefer [4] utilize the time integral of the ripple voltage method for obtaining ripple current.

The angle β must be first be calculated using (10).

$$\beta = \arcsin \left[\frac{E_d}{E_m} \right] = \arcsin \left[\frac{E_d}{1.047E_{do}} \right] \quad (10)$$

The time integral of the ripple voltage can then be calculated using (11). If:

$$\alpha + \mu \geq \beta - \frac{\pi}{3}, \quad (11)$$

Then:

$$\int edt = \frac{1047.2E_{do}}{\omega} \left[\cos \left(\alpha + \mu + \frac{\pi}{3} \right) + \cos \beta - \left(\frac{2\pi}{3} - \beta - \alpha - \mu \right) \sin \beta \right],$$

If $\alpha + \mu \leq \beta - \frac{\pi}{3}$,

Then:

$$\int edt = \frac{1047.2E_{do}}{\omega} [2 \cos \beta - (\pi - 2\beta) \sin \beta].$$

To obtain the current ripple the time integral of voltage is divided through by the converter output load inductance in mH per (12).

$$\Delta i = \frac{\int edt}{\text{mH}} \quad (12)$$

E. Dobinson Method

Dobinson arrives at the following expressions to calculate the per unit harmonic source currents. [1] [8]

$$\frac{I_h}{I_1} = \left[\frac{1}{h} + \frac{6.46r}{h-1} - \frac{7.13r}{h} \right] (-1)^k \text{ for } h = 6k - 1 \quad (13)$$

$$\frac{I_h}{I_1} = \left[\frac{1}{h} + \frac{6.46r}{h+1} - \frac{7.13r}{h} \right] (-1)^k \text{ for } h = 6k + 1$$

Where:

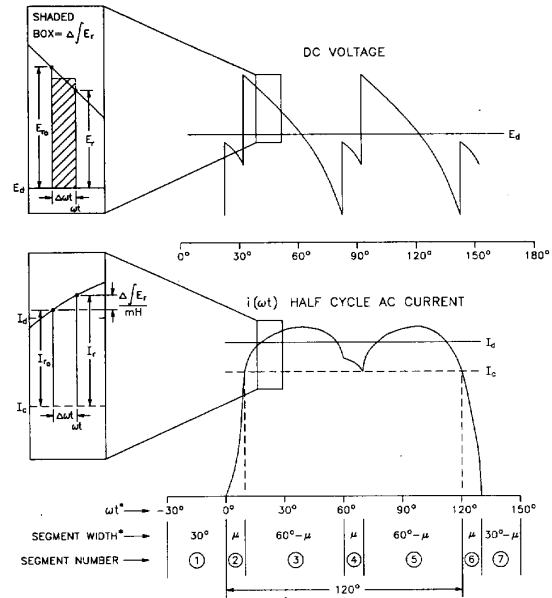
$$r = \frac{\Delta i}{I_d}$$

F. Graham-Schonholzer Method

The commutation current I_c must be calculated according to (14) and then the ripple coefficient according to (15). [2]

$$I_c = I_d - \Delta i \left[\frac{2 \sin(\pi/6 - \mu/2) - (\pi/3 - \mu) \sin(\pi/3 + \mu/2)}{(\pi/3)(1 - \sin(\pi/3 + \mu/2))} \right] \quad (14)$$

$$r_c = \frac{\Delta i}{I_c} \quad (15)$$



* SHOWN IN DEGREES - RADIAN USED IN CALCULATIONS
IN THIS NUMERICAL MODEL SCALING, WAVE RISES FROM AXIS AT 0 FOR ALL FIRING ANGLE

Fig. 7. Illustration of calculation method to setup current waveform for FFT analysis.

The per unit harmonic magnitudes of order $h = 6k + \text{or} - 1$ can then be calculated using (16).

$$\frac{I_h}{I_1} = \frac{2\sqrt{2}}{\pi} \left[\frac{\sin(h\pi/3) \sin(h\mu/2)}{h^2 \mu/2} + \frac{r_c g_h \cos(h\pi/6)}{1 - \sin(\pi/3 + \mu/2)} \right] \quad (16)$$

Where:

$$g_h = \left[\frac{\sin((h+1)(\pi/6 - \mu/2))}{h+1} + \frac{\sin((h-1)(\pi/6 - \mu/2))}{h-1} - \frac{2 \sin(h(\pi/6 - \mu/2)) \sin(\pi/3 + \mu/2)}{h} \right]$$

G. FFT Method

This method is a software implemented numerical analysis procedure which constructs the actual ac current waveform in the time domain and then calculates the Fast Fourier Transform (FFT) to arrive at the constituent harmonics. Rather than using a single Voltage integral divided by inductance quantity applicable twice each half cycle and assuming sine wave shaped humps as in the other methods, an incremental step-by-step integration procedure constructs the actual current wave. Fig. 7 illustrates this procedure for a positive half cycle of the current wave which is divided into seven different segments.

The equations for each segment are defined below. These equations describe the current $i(\omega t)$ for ωt from 0 to 180 degrees.

Segment 1

$$i(\omega t) = 0 \quad (17)$$

Segment 2

$$i(\omega t) = I_c \left(\frac{\cos \alpha - \cos(\alpha + \omega t)}{\cos \alpha - \cos(\alpha + \mu)} \right) \quad (18)$$

Segment 3 The equations for Segments 1 and 2 produce the magnitude of $i(\omega t)$ for any discrete value of ωt . To calculate the first of the double humps, the segment must be divided into a number of intervals and a sequential integration procedure performed across the width of the segment as illustrated for one of the intervals in the expanded portions of Fig. 7. For each integration interval the following set of equations can be used to determine a set of $i(\omega t)$ across the width of the hump.

The instantaneous dc ripple voltage is first calculated using:

$$e_r(\omega t) = \sqrt{2}E_{LL} \sin(\pi/3 + \alpha + \omega t) - E_d \quad (19)$$

The incremental change in current which is the integral of voltage divided by the converter output inductance can then be calculated using (20).

$$\frac{\Delta \int E_r}{\text{mH}} = \left(\frac{\Delta \omega t}{2\pi f} \right) \left(\frac{E_r + E_{r_o}}{2} \right) \left(\frac{1000}{\text{mH}} \right) \quad (20)$$

Finally, (21) and (22) can be utilized to calculate the ripple current and the total ac current value.

$$I_r = I_{r_o} + \frac{\Delta \int E_r}{\text{mH}} \quad (21)$$

$$i(\omega t) = I_c + I_r \quad (22)$$

Segment 4 The calculation procedure for this commutation interval is the same as that for Segment 3 except that (23) should be utilized to calculate the ripple voltage.

$$e_r(\omega t) = \frac{\sqrt{2}E_{LL}(\sin(\alpha + \omega t) + \sin(\pi/3 + \alpha + \omega t))}{2} - E_d \quad (23)$$

Equations (20), (21) and (22) are then used.

Segment 5 The calculation procedure for the second hump is the same as that for Segment 3 except that (24) should be utilized to calculate the ripple voltage.

$$e_r(\omega t) = \sqrt{2}E_{LL} \sin(\alpha + \omega t) - E_d \quad (24)$$

Equations (20), (21) and (22) are then used.

Segment 6

$$i(\omega t) = I_c \left(1 - \frac{1 - \cos(\omega t - 2\pi/3)}{1 - \cos \mu} \right) \quad (25)$$

Segment 7

$$i(\omega t) = 0 \quad (26)$$

In order to determine the commutating current I_c , the average dc value of the ripple current calculated with the above equations must be subtracted from the total I_d . Boundary values between the segments must be calculated and factored as well into the numerical procedure. To obtain a full cycle of values, the negative values should be used for the negative half cycle function. The even harmonics generated by asymmetrical SCR firing can easily be determined by generating a different waveform for the negative half-cycle.

Having constructed the current waveform in the time domain, the final step is to use numerical procedures to take the FFT of the function in order to obtain the constituent harmonic values of the waveform.

REFERENCES

- [1] L. G. Dobinson, "Closer Accord on Harmonics," *IEE Electron. Power*, pp. 567, May 1975.
- [2] A. D. Graham and E. T. Schonholzer, "Line Harmonics of Converters with DC-Motor Loads," *IEEE Trans. Industry Applic.*, vol. IA-19, no. 1, pp. 84-93, January/February 1983.
- [3] IEEE Std. 519-1992, "IEEE Recommended Practices and Requirements for Harmonic Control in Electrical Power Systems," April, 1993.
- [4] J. Schaefer, *Rectifier Circuits: Theory and Design*. New York: Wiley, 1965.
- [5] J. Arrillaga, J. F. Eggleston and N. R. Watson, "Analysis of the AC Voltage Distortion Produced by Converter-Fed DC Drives," *IEEE Trans. Industry Applic.*, vol. IA-21, no. 6, pp. 1409-1417, November/December 1985.
- [6] J. S. Ewing, "Lumped Circuit Impedance Representation for dc Machines," *IEEE Trans. Power Applic. Syst.*, vol. PAS-87, pp. 1106-1110, 1968.
- [7] E. W. Kimbark, *Direct Current Transmission Volume I*. New York: Wiley, 1971.
- [8] J. Arrillaga, D. A. Bradley and P. S. Bodger, *Power System Harmonics*. Wiley, 1985.



David E. Rice (M'78) received the B.S.E.E. degree from Union College, Schenectady, NY, USA, in 1972. He joined the General Electric Company in 1973 and after engineering assignments in Los Angeles, Philadelphia, and Schenectady he became an Application Engineer in Houston, TX, involved in the system application of electrical generation, distribution, and drive equipment. He is presently a Senior Power System Engineer with responsibility for conducting various types of analytical studies on electrical power systems.